Eur. Phys. J. B **64**, 433–436 (2008)
DOI: 10.1140/epjb/e2008-00079-y

THE EUROPEAN PHYSICAL JOURNAL B

Inertial capture in flow through porous media

J.S. Andrade Jr.[a], A.D. Araújo, T.F. Vasconcelos, and H.J. Herrmann

Departamento de Física, Universidade Federal do Ceará, 60451-970 Fortaleza, Ceará, Brazil

Received 21 September 2007 / Received in final form 28 January 2008
Published online 27 February 2008 –

Abstract. We investigate through numerical calculation of non-Brownian particles transported by a fluid in a porous medium, the influence of geometry and inertial effects on the capture efficiency of the solid matrix. In the case of a periodic array of cylinders and under the action of gravity, our results reveal that $\delta \sim St$, where δ is the particle capture efficiency, and St is the Stokes number. In the absence of gravity, we observe a typical second order transition between non-trapping and trapping of particles that can be expressed as $\delta \sim (St - St_c)^{\alpha}$, with an exponent $\alpha \approx 0.5$, where St_c is the critical Stokes number. We also perform simulations for flow through a random porous structure and confirm that its capture behavior is consistent with the simple periodic model.

PACS. 47.56.+r Flows through porous media – 47.55.Kf Particle-laden flows – 05.70.Jk Critical point phenomena – 83.80.Hj Suspensions, dispersions, pastes, slurries, colloids

1 Introduction

The relevant aspects for the comprehension of fluid flow and particle transport in an irregular geometry are the *structural* one, associated to the topological and morphological conformation of the porous media, and the *phenomenological* one, that refers to the hydrodynamics and particle movement and capture mechanisms. For instance, the concept of hydrodynamic dispersion commonly refers to the band broadening phenomenon observed when a solute at low concentratin (ideal massless tracer) spreads along the pore space under the action of convection and molecular diffusion [1–3]. In this case, the effect of inertia on the movement of the tracer molecules is always considered negligible. However, the inertia on the transport of non-Brownian particles through flow in porous media certainly constitutes an important mechanism that is still quantitatively not very well understood [4]. It is usually quantified by the dimensionless *Stokes number*, $St \equiv V d_p^2 \rho_p / 18 \ell \mu$, where d_p and ρ_p are the diameter and density of the particle, respectively, ℓ is a characteristic length of the pores, μ is the viscosity and V is the velocity of the fluid.

Filtration is not only the basic mechanism to get clean air or water but also plays a crucial role in the chemical industry. For this reason it has been studied extensively in the past [5]. In particular, we will focus here on deep bed filtration where the particles in suspension are much smaller than the pores of the filter which they penetrate until being captured at various depths. For non-Brownian particles, at least four capture mechanisms can be distinguished, namely, the geometrical, the chemical, the gravitational and the hydrodynamical process [5]. In the past, very carefully controlled laboratory experiments were conducted by Ghidaglia et al. [6] evidencing a sharp transition in particle capture as a function of the dimensionless ratio of particle to pore diameter characterized by the divergence of the penetration depth. Using a capillary network to model the pore space morphology, they showed that this transition does not belong to the universality class of percolation, contrary to what simple geometrical considerations would suggest. Subsequently, Lee and Koplik [7] found a transition from an open to a clogged state of the porous medium that is a function of the mean particle size. Much less effort, however, has been dedicated to quantify the effect of inertial impact on the efficiency of a deep bed filter. For example, Ghidaglia et al. [6] only included this effect heuristically in their model through an *ad hoc* particle capture parameter. In this paper we investigate the inertial capture of non-Brownian particles in a porous medium. For this problem, which is closely related with deep bed filtration, we reveal novel scaling relations for ordered as well as random porous structures.

2 Inertial capture in a periodic porous medium

As shown in Figure 1, we start with an infinite ordered porous medium that can be completely represented in terms of a single square cell of unitary size ($L = 1$) and porosity given by $\epsilon \equiv (1 - \pi D^2/4)$, where D is the diameter of the obstacle. Assuming Stokesian flow, the streamfunction ψ is given by the linear biharmonic equation,

[a] e-mail: soares@fisica.ufc.br

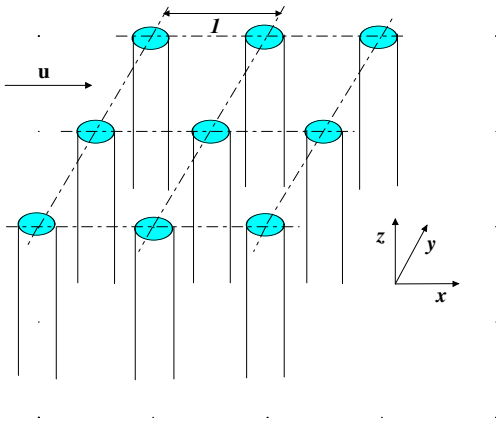

Fig. 1. Schematic representation of an ordered filter composed of a periodic array of cylinders.

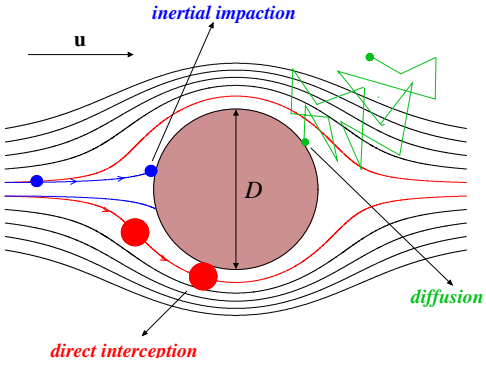

Fig. 2. Trajectories of particles released from different positions at the inlet of the periodic porous medium cell. Also shown are three possible capture mechanisms, among which only inertial impaction is considered in our study. The particles are dragged according to equation (1) and the flow field **u** is calculated from the analytical solution of Marshall et al. [8].

$\nabla^4\psi = 0$. Here we use the solution provided by Marshall et al. [8] to obtain the velocity flow field **u** and study the transport of particles numerically. For simplicity, we assume that (i) the particles are point-like; (ii) the influx of suspended particles is so small that the fluid phase is not affected by changes in the particle volume fraction, and (iii) particle-particle interactions are negligible. Finally, if we consider that the drag force and gravity are the only relevant forces acting on the particles, their trajectories can be calculated by integration of the following equation of motion:

$$\frac{d\mathbf{u}_p^*}{dt^*} = \frac{(\mathbf{u}^* - \mathbf{u}_p^*)}{St} + F_g \frac{\mathbf{g}}{|\mathbf{g}|} , \qquad (1)$$

where $F_g \equiv (\rho_p - \rho)\ell|\mathbf{g}|/(V^2\rho_p)$ is a dimensionless parameter, $\mathbf{g}$ is gravity, t^* is a dimensionless time, and $\mathbf{u}_p^*$ and $\mathbf{u}^*$ are the dimensionless velocities of the particle and the fluid, respectively. In Figure 2 we show trajectories calculated for particles released in the flow for $St = 0.25$. Once a particle touches the boundary of the obstacle, it gets trapped. Our objective here is to search for the position y_0 of release at the inlet of the unit cell ($x_0 = 0$) and above the horizontal axis, below which the particle is always captured and above which the particle can always escape from the system. The particle capture efficiency then can be straightforwardly defined as $\delta \equiv 2y_0$. In the limiting case where $St \to \infty$, since the particles move ballistically towards the obstacle, the particle efficiency reaches its maximum, $\delta = D$. For $St \to 0$, on the other hand, the efficiency is smallest, $\delta = 0$. In this last situation, the particles can be considered as tracers that follow exactly the streamlines of the flow, avoiding trapping at the solid matrix of the porous medium. In Figure 3, we show the log-log plot of the variation of δ/D with the rescaled Stokes number in the presence of gravity for three different porosities. In all cases, the variable δ increases linearly with St to subsequently reach a crossover at $St_\times$, and finally approach its upper limit ($\delta = D$). The results of our simulations also show that $St_\times \sim (\epsilon - \epsilon_c)$, where ϵ_c corresponds to the minimum porosity below which the distance between inlet and obstacle is too small for a massive particle to deviate from the obstacle. The collapse of all data confirms the validity of this simple rescaling approach. The inset on the bottom of Figure 3 shows that the behavior of the system in terms of particle capture becomes significantly different in the absence of gravity. The efficiency δ remains equal to zero up to a certain critical Stokes number, St_c, that corresponds to the maximum value of St below which particles cannot be captured, regardless of the position y_0 at which they have been released. Some evidence for such a finite critical point has been presented in previous analytical and numerical studies [9]. Right above St_c, the variation of δ can be described in terms of a power-law, $\delta \sim (St - St_c)^\alpha$, with an exponent $\alpha \approx 0.5$. In the inset on the top we show the variation of δ/D with the Stokes number for different values of gravity. For any finite value of g, we find a finite efficiency for positive Stokes numbers. Only for the zero gravity case the capture efficiency vanishes at a finite Stokes number St_c.

3 Filtering in a disordered medium

A more realistic model for the porous structure must include disorder [13]. Here we adopt a random pore space geometry that is often used to describe porous media [10]. It consists of non-overlapping circular obstacles of diameter D, separated by a distance larger than $D/10$, that are randomly allocated in a two-dimensional channel of width h, until a prescribed void fraction ϵ is reached. For compatibility between periodic and disordered descriptions, we take the characteristic pore size to be $\ell \equiv D/20$ (i.e., half of the minimum distance between any two obstacles of the disordered system). To reduce finite-size effects, periodic boundary conditions are applied in the y-direction. Finally, end effects of the flow field are reduced by attaching a header (inlet) and a recovery (outlet) region to the two opposite faces of the channel. The mathematical description for the fluid mechanics in the interstitial porous space is based on the Navier-Stokes and continuity equations [11]. In our simulations, we consider non-slip boundary conditions along the entire solid-fluid interface, and a

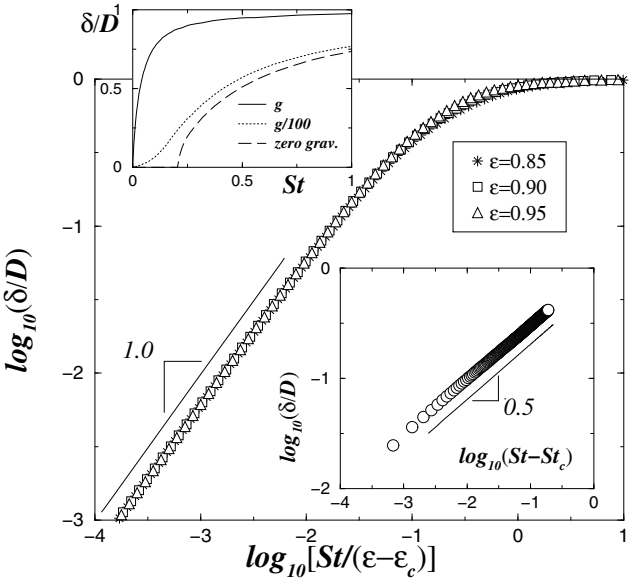

Fig. 3. Dependence of the capture efficiency δ on the rescaled Stokes number $St/(\epsilon - \epsilon_c)$ for periodic porous media in the presence of gravity. Here we use $F_g = 16$, a value that is compatible with the experimental setup described in reference [6]. The inset on the bottom shows that the behavior of the system without gravity can be characterized as a second order transition, $\delta \sim (St - St_c)^{\alpha}$, with $\alpha \approx 0.5$ and $St_c = 0.2096 \pm 0.0001$ for $\epsilon = 0.9$. The inset on the top shows the normalized capture efficiency δ as function of the Stokes number St for different values of gravity.

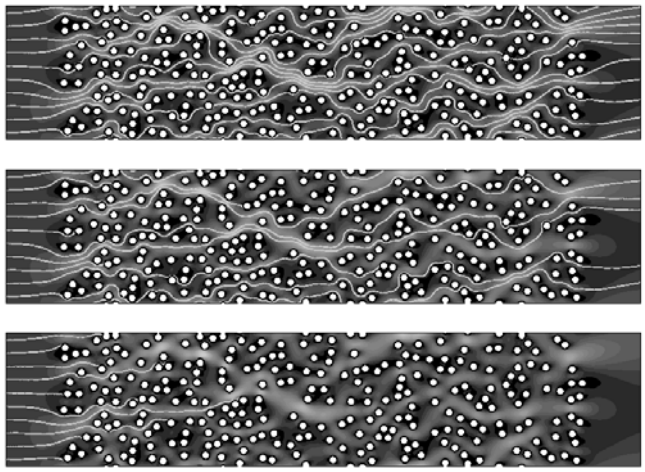

Fig. 4. (a) Contour plot of the velocity magnitude for a typical realization of a pore space ($\epsilon = 0.7$) subjected to low Reynolds conditions. Fluid is pushed from left to right. The colors ranging from dark to light gray correspond to low and high velocity magnitudes, respectively. Also shown are typical trajectories of particles in the flow through the porous medium, with gravity in the positive x-direction. From top to bottom the Stokes number is $St = 3.26 \times 10^{-4}$, 3.26×10^{-3} and 3.26×10^{-2}.

uniform velocity profile, $u_x(0, y) = V$ and $u_y(0, y) = 0$, is imposed at the inlet of the channel. The Reynolds number is defined as $Re \equiv \rho V h/\mu$. For simplicity, we restrict our study to the case where the Reynolds number is sufficiently low ($Re < 1$) to ensure a laminar viscous regime for fluid flow. The numerical solution for the velocity and pressure fields in the pore space is obtained through discretization by means of the control volume finite-difference technique [12].

Once the velocity and pressure fields are obtained for the flow in the pore space, we proceed with the calculation of particle transport. When the relative velocity is low $|\mathbf{u} - \mathbf{u}_p| \ll 1$, the relation between the particle and the fluid densities is high, $\rho_p/\rho \gg 1$, and $d_p > 1$ μm, except for the drag force and gravity, most of the forces acting on the particles become negligible [14]. The trajectories of the particles are calculated by numerical integration of their equations of motion. As in the periodic medium (see Eq. (1)), the gravity term is also included here, but we now consider a drag coefficient which is based on the empirical relation proposed by Morsi and Alexander [15].

In Figures 4a–4c we show typical trajectories of particles that have been released at the inlet of the porous system for $St = 3.26 \times 10^{-4}$, 3.26×10^{-3} and 3.26×10^{-2}. For a fixed value of St, we consider up to 1000 particles to determine (i) whether or not these particles get trapped and (ii) the precise position at the surface of the porous matrix where their capture takes place. From these positions, we obtain the profiles of the fraction of non-captured particles ϕ against the longitudinal distance x along the channel. In the limiting case of a very dilute system ($\epsilon \approx 1$) with particles being transported in the ballistic regime ($St \to \infty$), it is easy to show that $\phi(x) = \exp(-x/\lambda)$, with a penetration length given by $\lambda = \pi D/4(1 - \epsilon)$. For low and moderate values of St, the behavior of $\phi(x)$ is still exponential, but λ now being a function of the Stokes number. We then postulate that the previous result can be generalized to any combination of ϵ and St as,

$$\lambda = \frac{\pi D^2}{4(1-\epsilon)\delta}, \tag{2}$$

where the length δ is the capture efficiency analogously defined as for the periodic porous medium. In this way, the penetration depth is inversely proportional to the capture efficiency.

As shown in Figure 5, the penetration length follows a power-law $\lambda \sim (St)^{-\alpha}$, with a scaling exponent $\alpha \approx 1$ that is, within the numerical error bars, the same for the three values of porosity investigated. Simulations performed for a different realization of the disordered porous medium resulted in the same exponent. This value is also consistent with the exponent found for the periodic case with gravity. As also shown in Figure 5, the penetration length of the particles in the random pore space can be generally expressed as $\lambda/D = \beta/St(1 - \epsilon)$, where ϵ is the porosity, D is the grain size, and the prefactor β is a characteristic constant for the capture process. This simple relation discloses a novel way to rescale the relevant variables in the filtering system that can be useful in practical applications.

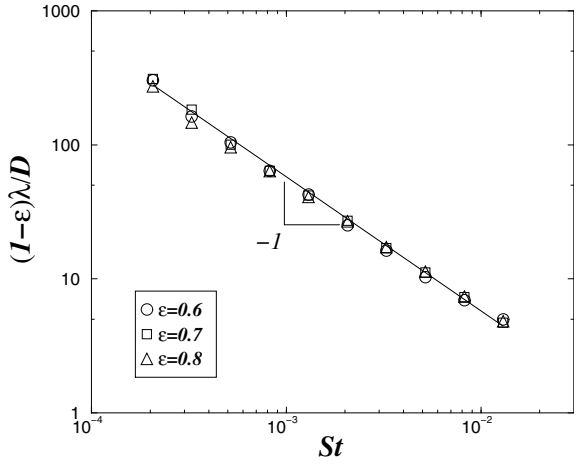

Fig. 5. Log-log plot showing the dependence of the rescaled penetration length $(1-\epsilon)\lambda/D$ on the Stokes number St for three different porosity values. The solid line corresponds to the best fit to the data of the scaling function $(1-\epsilon)\lambda/D = \beta St^{-\alpha}$ with the prefactor $\beta \approx 0.058$ and the exponent $\alpha = 1.00 \pm 0.02$.

4 Conclusion

In summary, we have studied the phenomenon of inertial capture of particles in two-dimensional periodic as well as random porous media. For the periodic model in the absence of gravity, there exists a finite Stokes number below which particles never get trapped. Furthermore, our results indicate that the transition from non-trapping to trapping with the Stokes number is of second order with a scaling exponent $\alpha \approx 0.5$. In the presence of gravity, we show that (i) this non-trapping regime is suppressed (i.e., $St_c = 0$) and (ii) the scaling exponent changes to $\alpha \approx 1$. Finally, the behavior of the random porous medium subject to gravity is shown to be consistent with this last picture. An interesting outcome from our results and their physical interpretation is the significant difference in behavior of the capture efficiency with Stokes number in the presence and in the absence of gravity. The scaling relations obtained from this analysis will be certainly useful to determine the microscopic role of the inertial capture mechanisms on the performance and design of filtering processes.

We thank CNPq, CAPES, FUNCAP and the Max-Planck prize for financial support.

References

1. J. Bear, *Dynamics of Fluids in Porous Materials* (Elsevier, New York, 1972)
2. F. A. Dullien, *Porous Media – Fluid Transport and Pore Structure* (Academic, New York, 1979)
3. M. Sahimi, *Flow and Transport in Porous Media and Fractured Rock* (VCH, Boston, 1995)
4. D.L. Koch, R.J. Hill, Annu. Rev. Fluid Mech. **33**, 619 (2001)
5. C. Tien, *Granular Filtration of Aerosols and Hydrosols* (Butterworths, Boston, 1989)
6. C. Ghidaglia, L. de Arcangelis, J. Hinch, E. Guazzelli, Phys. Rev. E **53**, R3028 (1996); C. Ghidaglia, L. de Arcangelis, J. Hinch, E. Guazzelli, Phys. Fluids **8**, 6 (1996)
7. J. Lee, J. Koplik, Phys. Fluids **13**, 1076 (2001)
8. H. Marshall, M. Sahraoui, M. Kaviany, Phys. Fluids **6**, 507 (1993)
9. L.M. Levin, Izdatel'stvo Academii Nauk SSSR (1961), *Eng. Transl. Foreing Techn. Div. Doc. No. FTD-HT-23-1593-67*; N.A. Fuchs, *The Mechanics of Aerosols* (Pergamon, New York, 1964); D.B. Ingham, L.T. Hildyard, M.L. Hildyard, J. Aerosol Sci. **21**, 935 (1990)
10. S. Torquato, *Random Heterogeneous Materials: Microstructure and Macroscopic Properties* (Springer-Verlag, New York, 2001)
11. A.D. Araujo, J.S. Andrade Jr, H.J. Herrmann, Phys. Rev. Lett. **97**, 138001 (2006)
12. S.V. Patankar, *Numerical Heat Transfer and Fluid Flow* (Hemisphere, Washington DC, 1980); the FLUENT (trademark of FLUENT Inc.) fluid dynamics analysis package has been used in this study
13. J.S. Andrade Jr, D.A. Street, T. Shinohara, Y. Shibusa, Y. Arai, Phys. Rev. E **51**, 5725 (1995); H.E. Stanley, J.S. Andrade Jr, S. Havlin, H.A. Makse, B. Suki, Physica A **266**, 5 (1999); J.S. Andrade Jr, U.M.S. Costa, M.P. Almeida, H.A. Makse, H.E. Stanley, Phys. Rev. Lett. **82**, 5249 (1999)
14. J.K. Comer, C. Kleinstreuer, C.S. Kim, J. Fluid Mech. **435**, 55 (2001)
15. S.A. Morsi, A.J. Alexander, J. Fluid Mech. **55**, 193 (1972)